American Journal of Astronomy and Astrophysics
2023; 10(2): 14-22
http://www.sciencepublishinggroup.com/j/ajaa
doi: 10.11648/j.ajaa.20231002.11
ISSN: 2376-4678 (Print); ISSN: 2376-4686 (Online)

The Study of the Photometry and Flare Analysis of Kepler Flare Candidate 2MASS J22285440-1325178

Muallim Yakubu[1], Chima Abraham Iheanyichukwu[1, *], Kassimu Abdullahi Anderson[2]

[1]Department of Industrial Physics, Enugu State University of Science and Technology, Enugu, Nigeria

[2]Department of Physics, Air Force Institute of Technology, Kaduna, Nigeria

Email address:

yakubumuallim@gmail.com (Muallim Yakubu), abraham.chima@esut.edu.ng (Chima Abraham Iheanyichukwu), aakassimu@yahoo.com (Kassimu Abdullahi Anderson)

[*]Corresponding author

To cite this article:

Muallim Yakubu, Chima Abraham Iheanyichukwu, Kassimu Abdullahi Anderson. The Study of the Photometry and Flare Analysis of Kepler Flare Candidate 2MASS J22285440-1325178. *American Journal of Astronomy and Astrophysics*. Vol. 10, No. 2, 2023, pp. 14-22. doi: 10.11648/j.ajaa.20231002.11

Received: August 7, 2023; **Accepted**: August 28, 2023; **Published**: September 18, 2023

Abstract: The photometry and flare analysis of Kepler flare candidate 2MASS J22285440- 1325178 has been presented. The light curve shows the amplitude distributions for the 2MASS J22285440-1325178. From the light curve, the shorter amplitude represents the short duration of the flares while the larger amplitude show the highest peak of the flares, with amplitude range duration from 7457.70-15482.7700 (e^-/sec). The magnitude of the flares varies with times (days) and the light curve, the plot of the light curve demonstrates the frequency of the flares and the range of the magnitude. The amplitude represents the flux peak of each flare, which indicates that flare stars have larger amplitudes and hence larger star spots than normal stars. Our data was obtained from the Milkulski Archive for Space Telescope (MAST). The instrument used for data analysis of 2MASS J22285440-1325178 candidate are python Jupiter notebook software package. In addition, aperture photometric reduction of 2MASS J22285440-1325178 at EPIC 206050032 have been carried out to obtain the light curve. Furthermore, flare amplitude was analyzed as well as the flare rise time and equivalent duration.

Keywords: Flares, Photometry, Amplitudes, Flux

1. Introduction

Flare stars are stars that brighten rapidly over a short period of time and are found in cool stars such as K, G, and M stars [1]. They are magnetically active [32]. A sharp intense outburst on the star surface caused by a magnetic reconnection from the inside to the exterior of a cool dwarf star causes the luminosity or abrupt brightness to be noticed in an observer's line of sight within a short amount of time [2]. This behavior is frequently observed in red dwarfs, which are smaller or similar in size to the Sun and have lower surface temperatures in the range of 4000 to 6000K than medium-sized or gigantic stars [3]. Because red dwarfs have low surface temperatures, their brightness is dim, and their brightness magnitudes are small, making them difficult to observe. During an outburst, however, the brightness magnitude or flux increases dramatically, allowing telescopes to identify them.

Photometry, in which the telescope measures the brightness magnitude, or spectroscopy, in which the flux is measured, are two methods of observation. Photometry is the science of determining the brightness of light as seen by the human eye [4]. Aperture photometry is a basic technique for measuring the brightness of an astronomical object, such as a star or galaxy, in astronomical picture data analysis.

It is the summation of observed counts from a sub-image including the source (or possibly sources) and subtraction of the sky background contribution calculated from a nearby imaged region that excludes the source of interest to calculate source intensity [5].

As a result of magnetic reconnection, flares appear on nearly all main sequence stars with outer convective envelopes [24, 25]. They are often found on low-mass stars with deep convection zones, such as M dwarfs, and occur stochastically. Solar flares are like planetary flares. Both are thought to form through the same mechanism: a magnetic reconnection event produces a beam of charged particles that collides with the stellar photosphere, causing rapid heating and the emission we see at nearly all wavelengths [6]. The strength of the stellar surface magnetic field influences the frequency and energy of flares. The Sun is a well-studied and well-known flare possibility [7]. On the Sun, reconnection occurs around a pair of sunspots or between groupings of spots. Due to a constant loss of angular momentum, the strength of a star's surface magnetic field weakens over time, quieting the internal dynamo [8, 9].

In layman's terms, a flare star is a brief increase in the brightness of a star; thus, flare stars are variable stars. A variable star is one whose brightness (or apparent size) changes as observed from Earth. The difference could be as small as a few parts per million, or it could be a thousand times larger. It could happen in a fraction of a second, or it could take years, decades, or millennia. These are extremes, but astronomers have devised a variety of methods for locating, measuring, and analyzing the complete range of variable stars.

Because the variances provide essential and often-unique information on the nature and evolution of the stars, this is the case. This data can be utilized to derive even more fundamental understanding about the cosmos. A shift in emitted light or anything partially obstructing the light, such as an exoplanet, might produce this variation [26]. As a result, the Kepler Mission's goal is to find Earth-size planets in the habitable zones of solar-type stars like F and K stars [10, 11], quantify their frequency, and characterize them. The preferred method is transit photometry, which reveals the planet's orbital period and size in relation to its star.

High photometric precision is required for transit photometry, which requires continuous time series data of many stars over a long period of time. Though Kepler was created with the goal of detecting terrestrial planets, the nature of Kepler data set makes it extremely useful for stellar astrophysics. Photometric study in astronomy is a way of observing a particular object by counting the number of photons emitted from a target in seconds using a charge couple devices (CCD) telescope [12, 13].

Searching archive data of 2MASS from the Kepler K_2 online database for photometric data of 2MASS J22285440-1325178 will be the next step (LP 760-3). On 2MASS J22285440-1325178 (LP 760-3), aperture photometric reduction will be done to produce a target pixel file and a light curve data, followed by data reduction to obtain the light curve and a series of analyses to estimate the flare parameters.

2. Data Source

The research data was collected from Milkulski Archive for Space Telescope (MAST), Kepler K_2 campaign 3 for studying the properties of 2MASS J22285440-1325178. The Milkulski Archive for Space Telescope (MAST) is a NASA funded project to support and provide to the astronomical community a variety of astronomical data archives, with the primary focus on scientifically related data sets in the optical, ultraviolet, and near-infrared parts of the spectrum. MAST is hosted by the Space Telescope Science Institute (STScI) in the United States. K_2 data for 2MASS J22285440-1325178 was sourced from the MAST online archive. The optical fits file data was downloaded from the (http://archive.stsci.edu/hlsps/polar/c03/206000000/49476/hlsp_polar_k$_2$_lightcurve_206049476-c03_kepler_v1_llc.fits.) A FITS (Flexible Image Transport System) is the data format most widely used within astronomy for transporting analyzing and archiving scientific data files.

2.1. Methods

The instrument used for data analysis and light curve of 2MASS J22285440-1325178 candidate are python Jupiter notebook software package which are meant to give out information objectively through their effective usage to produce results. This work follows series of methods, which are described in this section.

2.2. Target Selection Tools

K_2fov Python package was used to identify the exact campaign the target enables the community to test whether targets fall within a campaign field the target 2MASS J22285440-1325178 falls in. Findings shows that the target was observed in K_2 campaign 3 whose sky field is shown in Figure 1. The following header properties were obtained from the header unit of the fits file.

Table 1. *Header Properties of 2MASS J22285440-1325178 from K_2 archive.*

PROPERTIES OF 2MASS J22285440-1325178 FROM K_2 ARCHIVE	VALUE
Observation Type	Science
Mission	K_2
Provenance Name	hlsp_polar
Instrument Name	Kepler
Project	hlsp_polar
Filters	Kepler
Waveband (wavelength region)	Optical
Target Name	polar206049476
Observation ID	polar206049476-c03_lc
RA (s_ra)	337.229925 (22:28:55.182)

PROPERTIES OF 2MASS J22285440-1325178 FROM K_2 ARCHIVE	VALUE
Dec (s_dec)	-13.436741 (-13:26:12.27)
Proposal ID	GO3051_GO3081
Product Type	Timeseries
Calibration Level	2
Object Kepler ID	EPIC 206050032
CCD channel	37
CCD module	12
CCD output	1
Observing campaign number	3
Data release version number	26
Observing mode	Long cadence
Target table ID	79
Reference frame of celestial coordinates	ICRS
Right ascension (deg)	337.226670
Declination (deg)	-13.421627
Equinox of celestial coordinate system	2000.0
J band magnitude from 2MASS (mag)	10.768
H band magnitude from 2MASS (mag)	10.217
K band magnitude from 2MASS (mag)	9.843
Kepler magnitude (Kp mag)	13.211
Start Time (t_min)	56976.5977806366 (2014-11-15 14:20:48)
End Time (t_max)	57045.7655296296 (2015-01-23 18:22:21)
Exposure Length (t_exptime)	5976093
Min. Wavelength (em_min)	418400000000
Max. Wavelength (em_max)	905000000000
S region	POLYGON ICRS 337.22764049 -13.43451900 337.22764044 -13.43896300 337.23220956 -13.43896300 337.23220951 -13.43451900
Data Rights	Public
Product Group ID	9700039452

2.3. Data Reduction

The fits data was reduced using Kepler photometric reduction tools available at https://archive.stsci.edu/missions-and-data/k2.

Aperture photometry was performed to obtain target pixel files. Target Pixel Files (TPFs) are files common to Kepler/K_2 and the TESS mission. They contain movies of the pixel data cantered on a single target star; in this case 2MASS J22285440-1325178. A Target Pixel File of 2MASS J22285440-1325178 is shown in Figure 2.

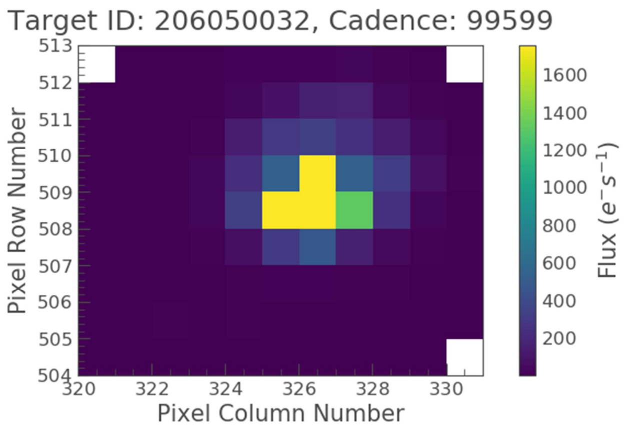

Figure 1. *Target Pixel File of 2MASS J22285440-1325178 shown the first frame as observed from the light curve.*

Each of the pixels are 4 arc seconds across. The point spread function (PSF) of the telescope causes the light from the star to fall onto several different pixels, which can be seen in the image above. Because of this spreading, there is need to sum up many pixels to collect all the light from the source. To do this, all the pixels in an aperture were summed up. An aperture is a pixel mask, where only the pixels related to the target are taken. The Kepler data reduction pipeline adds an aperture mask to each target pixel file. This aperture determines which pixels are summed to create a 1-D light curve of the target. Figure 3 shows the target pixel file with its aperture mask.

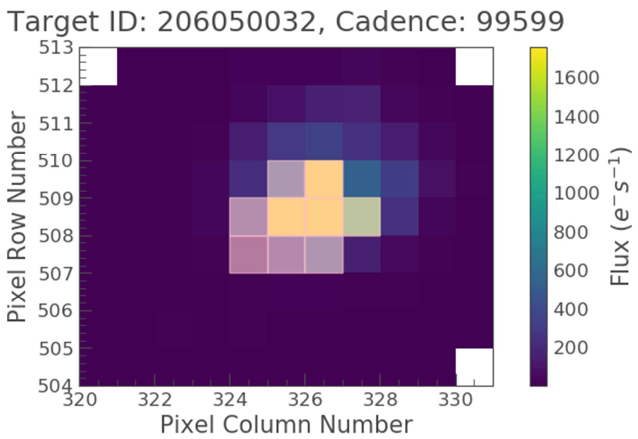

Figure 2. *Target Pixel File of 2MASS J22285440-1325178 with its mask.*

3. Result

A plot of flux (e^{-}/sec) against time (days) is shown in the light curves of the flare period, amplitude, flare rise time and equivalent duration of 2MASS J22285440-1325178.

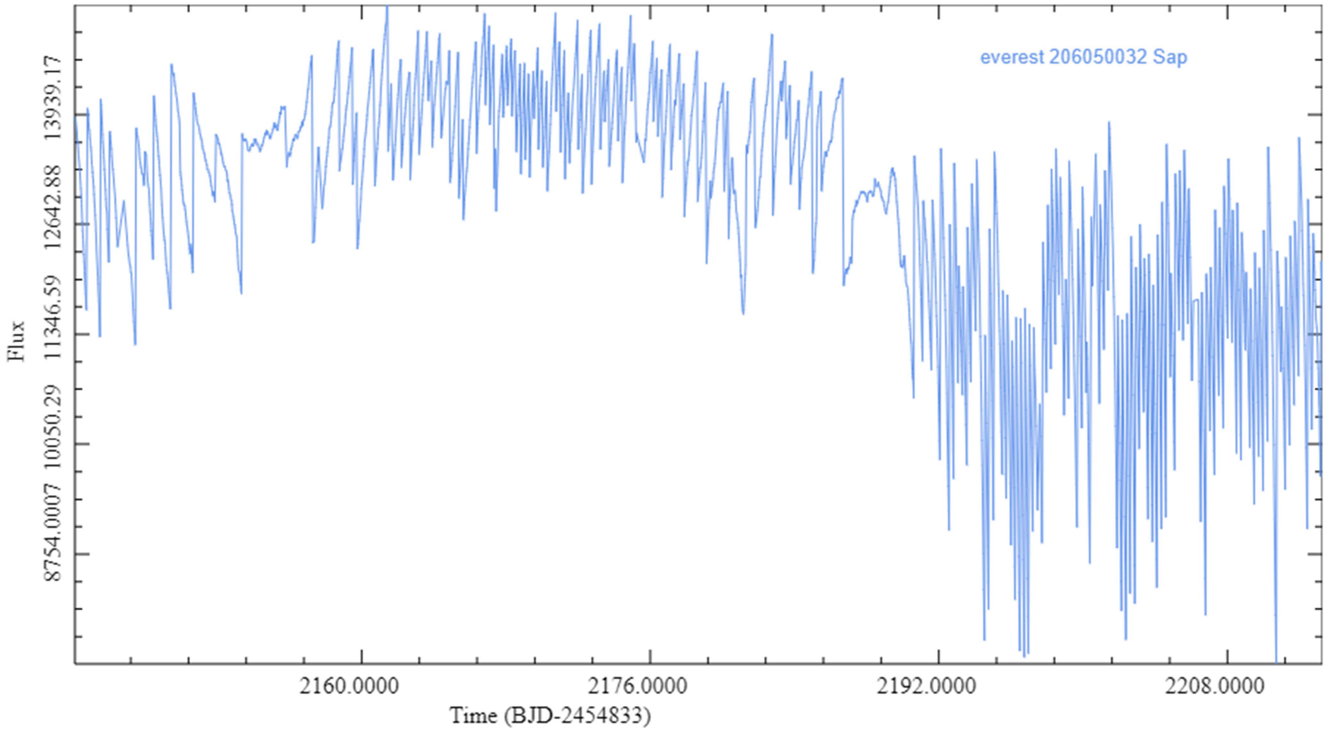

Figure 3. *The Light curve of the flare period, amplitude, flare rise time and equivalent duration of 2MASS J22285440-1325178 observed at EPIC 206050032 by Kepler K_2 campaign 3. Min flux: 7457.7085, max flux: 15482.7700, flux range: (e^{-}/sec) 7457.7085 to 15482.7700.*

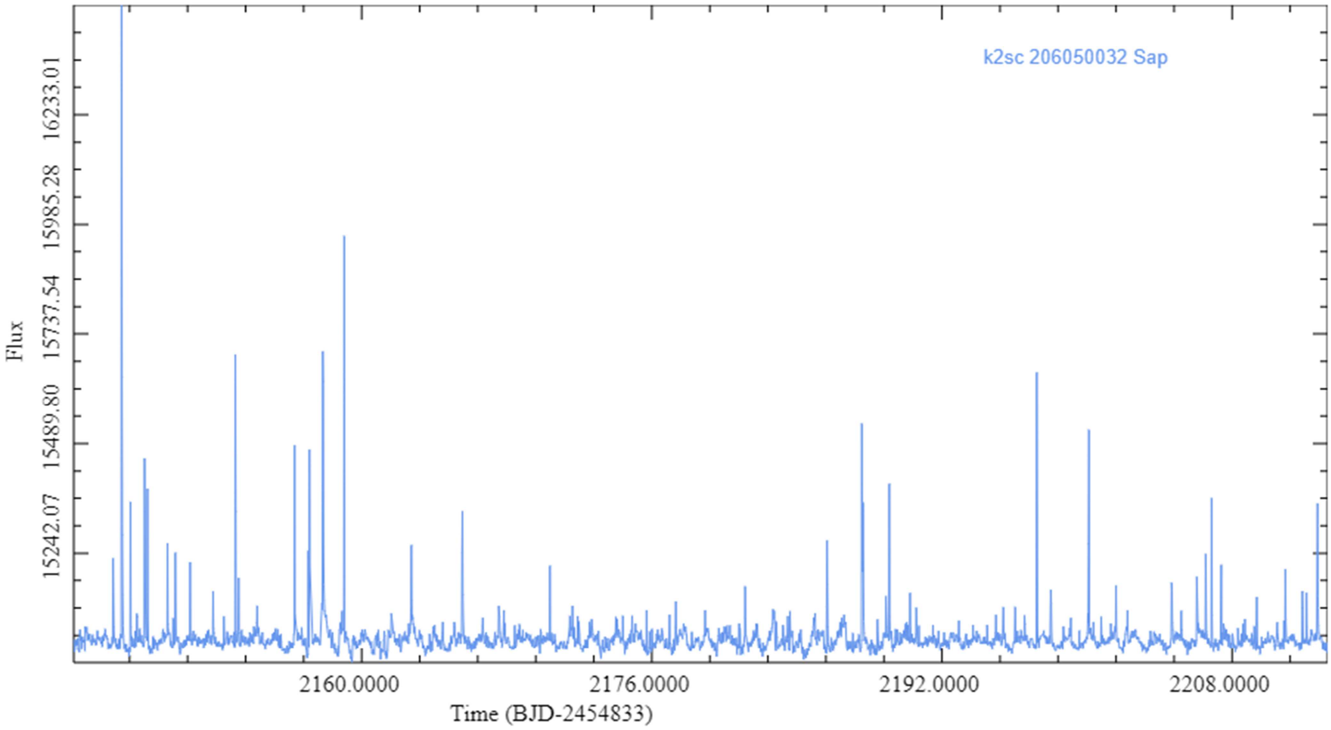

Figure 4. *The Light curve of the flare period, amplitude, flare rise time and equivalent duration of 2MASS J22285440-1325178 observed at EPIC 206050032 by Kepler K_2 campaign 3. Min flux: 14994.3330, max flux: 16480.7480, flux range: (e^{-}/sec) 14994.1235 to 16480.7480.*

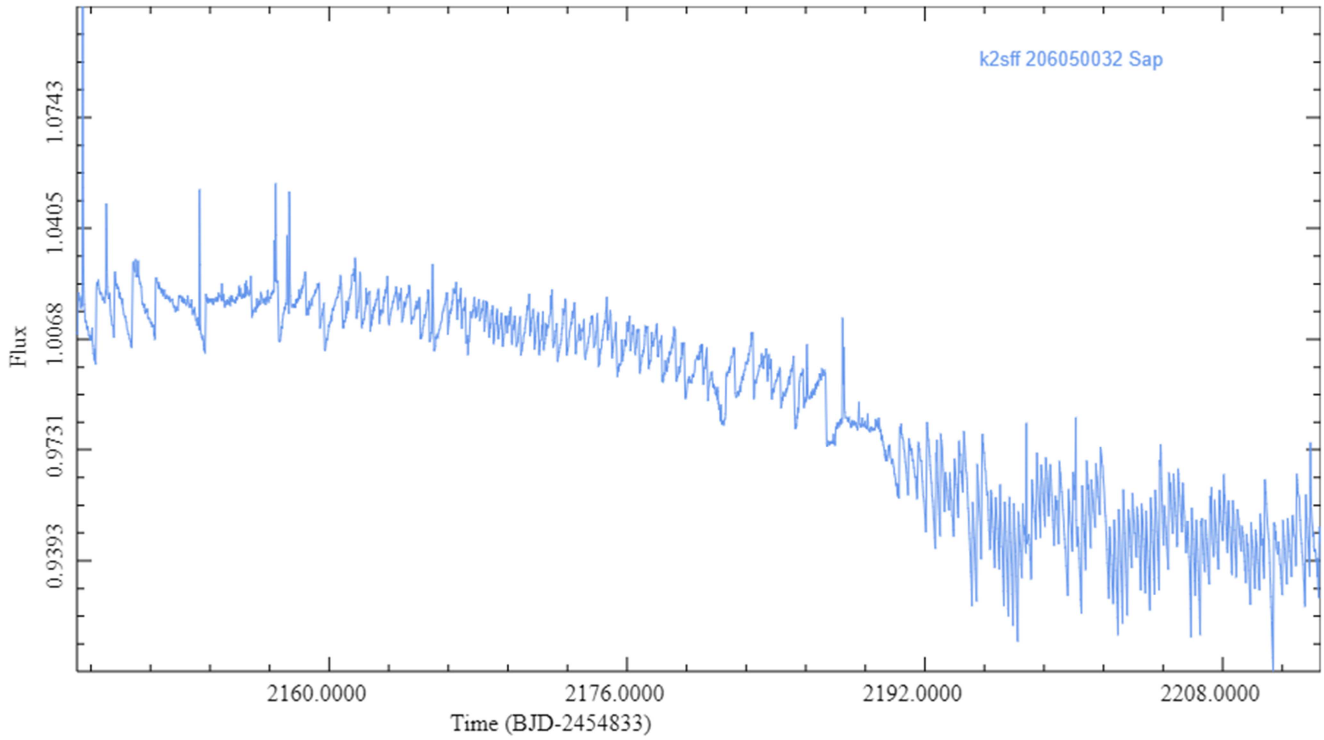

Figure 5. *The Light curve of the flare period, amplitude, flare rise time and equivalent duration of 2MASS J22285440-1325178 observed at EPIC 206050032 by Kepler K_2 campaign 3. Min flux: 0.9056, max flux: 1.1080, Flux range (e-/sec): 0.9567 to 1.1080.*

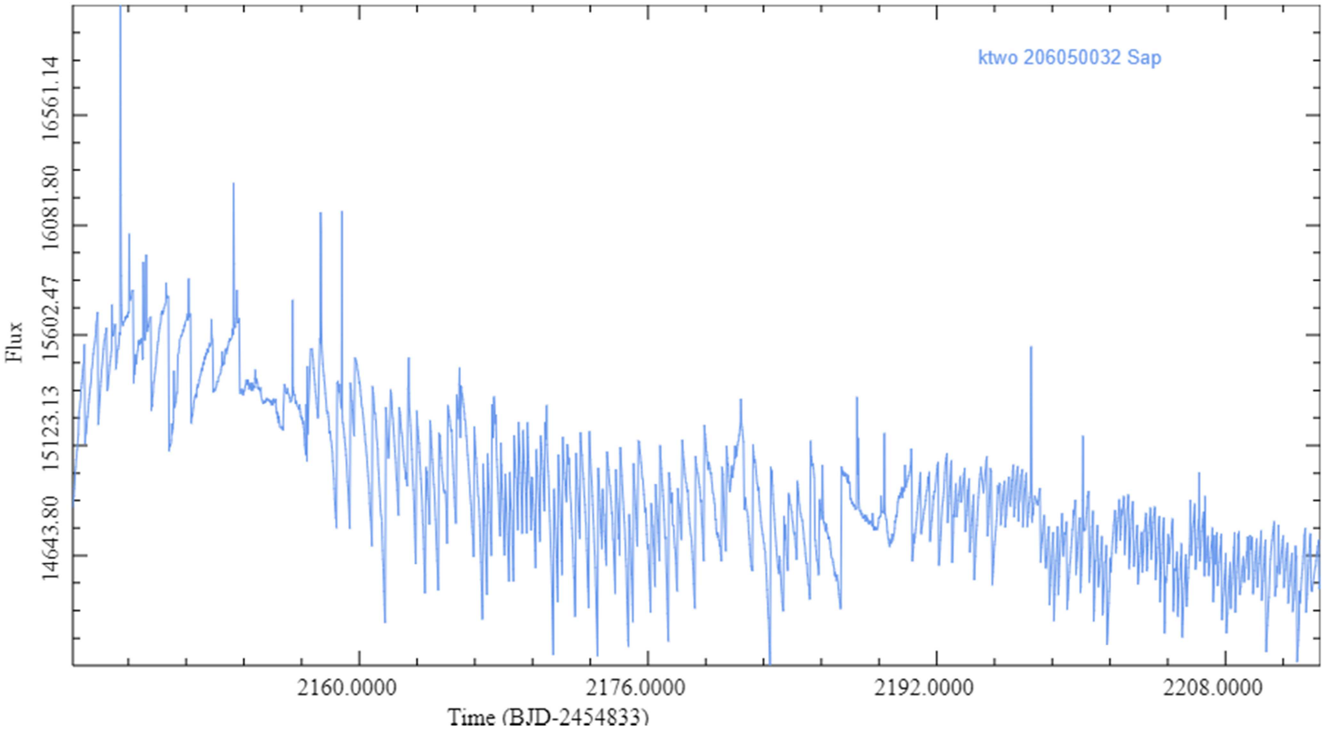

Figure 6. *The Light curve of the flare period, amplitude, flare rise time and equivalent duration of 2MASS J22285440-1325178 observed at EPIC 206050032 by Kepler K_2 campaign 3. Min flux: 14164.4619, max flux: 17040.4727, Flux range (e-/sec): 14164.4619 to 17040.4727.*

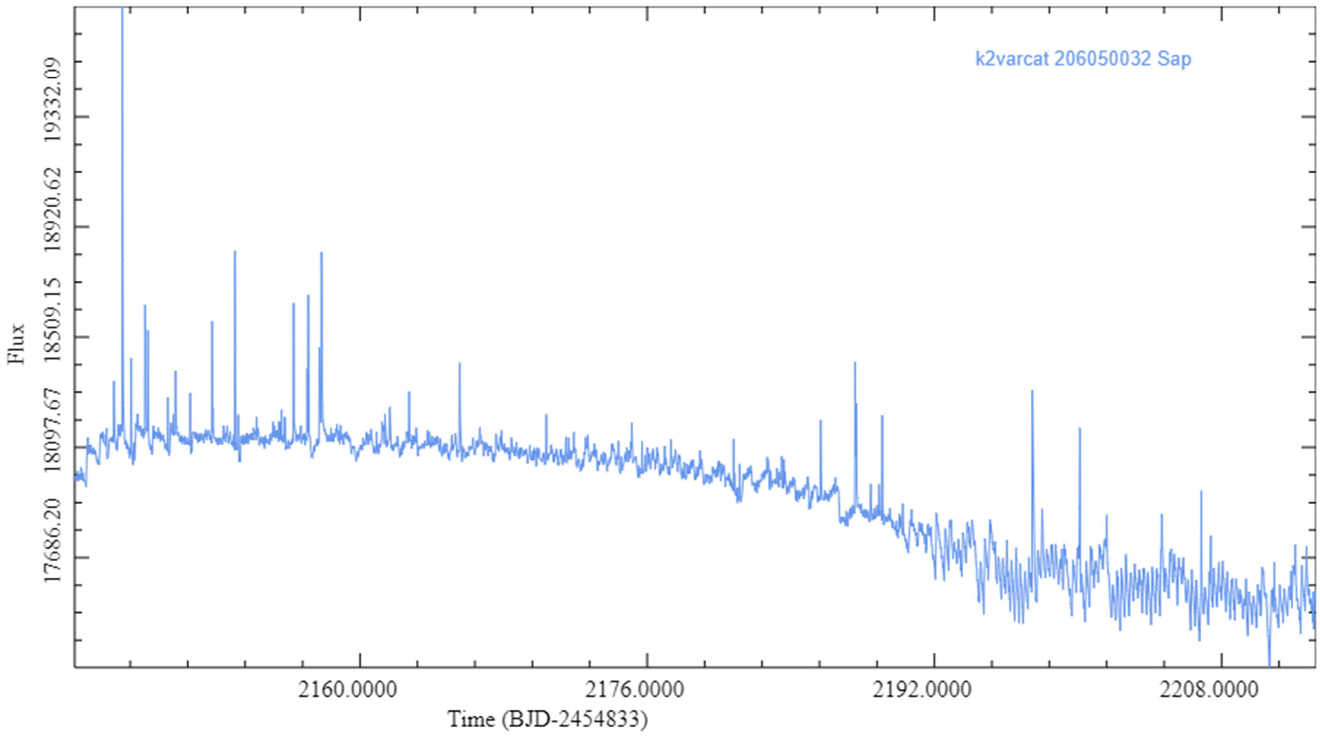

Figure 7. *The Light curve of the flare period, amplitude, flare rise time and equivalent duration of 2MASS J22285440-1325178 observed at EPIC 206050032 by Kepler K_2 campaign 3. Min flux: 17274.7285, max flux: 19743.5664, Flux range (e-/sec): 17274.7285 to 19743.5664.*

Table 2. *The Light curve of the flare period, amplitude, flare rise time and equivalent duration of 2MASS J22285440-1325178 observed at EPIC is presented in the table below.*

EPIC ID	Rotation period (Prot) d	Min flux Duration (e^-/sec)	Max flux Duration (e^-/sec)	Amplitude Flux Range (e^-/sec)
206050032	>70.00	14835.62	15482.77	7457.70-15235.46

3.1. Discussion

I have analyzed flaring activity from a sample of 2MASS J22285440-1325178 covering a range of spectral types, using K_2 SC data, placed lower limits on the rotation periods of 2MASS J22285440-1325178 using the K_2 light curves. In addition to this, I used the flare characteristics (energy, duration, and phase of the rotation cycle) to compute a statistical analysis of flares of this sample. It is known, from previous studies, [14, 15, 17], that faster rotating stars show greater flaring activity and the activity drops for stars with rotation periods >10 d.

In figure 3, the light curve which shows the amplitude distributions for the 2MASS J22285440-1325178 is displayed, the magnitude of the flares varies with times (day) and the light curve plot demonstrating the frequency of the flares and the range of the magnitude. The amplitude represents the flux peak of each flare, certainly indicates that flare stars have larger amplitudes and hence larger star spots. The situation for individual effective temperature ranges is not as clear, but one can indeed conclude that there is a tendency for flare stars to have larger spots (larger amplitudes) than non-flare stars.

The effective data and radii in the KIC were used to obtain the approximate light curve. Therefore, nothing can be inferred about the occurrence of flares on the 2MASS J22285440-1325178. Clearly, nearly all flares detected by Kepler have amplitudes more than 500 ppm.

Figure 4 shows the Light curve of the flare. Clearly, rotation plays an important role in generating flares, but this role may be indirect. Rotation is a measure of the age of the star [31, 33], and young stars are more active [34]. Although most flares show a sharp rise and an exponential decay, a significant proportion (about one-third) exhibit a bump on the decaying branch or else a sharp change in decay rate. The significance of this flare morphology is not clear since the stars with low surface gravities tend to have flares of longer duration. This is probably related to the differences in heat transport that occurs in stars with different atmospheric densities. The flare energy is strongly correlated with stellar luminosity and with stellar radius. The flare energy correlates with the cube of the stellar radius which can be understood if the typical loop length of a flare is roughly proportional to the stellar radius. In other words, the larger the star, the larger the active area. The amplitude represents the flux peak of each flare.

Figure 5, Flare light curves typically show a rapid rise to a sharply peaked maximum followed by a relatively slow decaying phase. The duration of an outburst is the period; the period varies with flares separated by several time (days) from the light curves. The variations of amplitude from the light curve result from flares. The timescales for flare rise and decay depends on the number of days, in searching for flares in the Kepler light curve. It is important to avoid instrumental effects as far as possible. There are, indeed, some features in the light curves of stars which resemble flares, but which occur at precisely the same time in every star. Such features are avoided since they are clearly not intrinsic to the star.

In Figure 6, the flare light curve shows the significant flares rise and the fluctuation of the brightness of the 2MASS J22285440-1325178 which shows flares variation with amplitude. The amplitude represents the flux peak of each flare in the light curve which varies with time (days) and that the variation of the brightness or flares is because of the rotation of the star. From the light curve, the shorter amplitude represents the short duration of the flares while the larger amplitude shows the highest peak of the flares. Rotation can produce change in brightness. The amplitude represents the flux peak of each flare all which were obtained from the output of flare by Eye (FBEYE).

Figure 7, shows the rotational phase of flares on 2MASS J22285440-1325178 which identified flaring activity and we indicated their observed rotation period; the number of flares together with their duration, amplitude, and energy. Since the length of each observation differs, We have included a normalized flare number which is the number of flares expected on each star if the observation duration was 80 d.

3.2. Flare Identification

The flare identification process was completed using Flares by eye (FBEYE), a suite of IDL programs created by [23]. FBEYE allows users to manually classify flares present in the light curve via an interactive display. We are therefore able to determine for each flare the peak time, start time, end time, flux peak, and equivalent duration. The light curves which we used for this process were complete, meaning all photometric points were used regardless of their quality flag due to potential flaring events having quality flags which are not zero. The EVEREST quality flags and FBEYE flare list were then compared directly to assess the likelihood of the flare being relevant. Any photometric point with quality flags which were a result of thruster firing or known instrumental effects were removed from further analysis. Any point which had a flag of EVEREST bits 23 and 25 (which may have been due to cosmic rays or a real stellar flares) were kept. Events which consisted of only one photometric point were removed and events which did not have profiles consistent with being a likely stellar flare (i.e. sharp rise and exponential decay) were also removed. The data for 2MASS J22285440-1325178 were analyzed in a consistent manner and show the number of flares, the range in the duration and amplitude of the flares in addition. We have added the normalized flare number which represents the number of flares expected on each star if the observation duration was 78.3d. The duration of each flare was calculated from the start and stop times and the amplitude represents the flux peak of each flare all which were obtained from the output of FBEYE which is in line with other authors [18, 19].

3.3. Rotational Phase

Stars with star spots can show a periodic change in brightness as the stars rotates due to the star spots being cooler than the surrounding photosphere. If stellar flares originate from the star spot, one might naively expect more flares would be seen at rotation minimum where the star spot is most visible [28, 29]. However, if a star has a low rotation angle (i.e. one of its rotation poles is close to being face on), spots near the pole would be visible at all phases, and flares would be seen at all rotation phases [27].

3.4. Rotation Period

I first set out to determine or constrain the rotation period from the K_2 data [16] shows that the method used to determine the rotation period is initially through the Lomb–Scargle (LS) periodogram. We define $\varphi = 0.0$ as the rotational phase where the flux is at a minimum and is first obtained by eye. For stars with a modulation period longer than 10 d, I derive the rotation period, Prot, from the LS periodogram and fold the light curve to obtain a phase folded light curve. For stars where Prot< 10d, first is to refine Prot, and the time T0, which defines the first minimum, by phasing and folding sections of the light curve taken from the start, middle, and end [20-22]. This procedure allows Prot and T0 to be determined more accurately than the LS periodogram alone. This gives us a mean folded light curve. The uncertainty on the rotation period is estimated by determining the full width at half max (FWHM) of the corresponding peak on the power spectrum.

4. Summary

The study of the photometry and flare analysis of Kepler flare candidate 2MASS J22285440-1325178 was carried out using the Kepler K_2 Mission campaign 3, data collected at EPIC 206050032 using Kepler space optical telescope. The aim was to investigate the period of the star, to analyses the flare amplitude, to find out the flare rise time and equivalent duration. Flare stars are stars whose brightness increases within a short period and are observed in cool stars particularly K, G and M stars [14]. They have strong magnetic activity [30]. The work is based on archived data obtained from the Kepler K_2 photometric observations of campaign 3. It was observed from 2014-11-15 14:20:48 UT to 2015-01-23 18:22:21 UT in long cadence (~30 minute) mode. The total observation time for this campaign is 80 days. A photometric reduction of 2MASS J22285440-1325178 was carried out from the data obtained at EPIC 206050032 which yielded 3192 good data points. The first 100 data points were used only to plots the light curves of the flares. All fluxes are in electron/seconds and time in Barycentric Kepler Julian Date.

Finally, the different light curves of flare activity of 2MASS J22285440-1325178 was plotted showing the peaked flux which is the amplitude, flare rise time and equivalent duration and as well as the rotation period.

5. Conclusion

Previous observations of flaring activity levels in fast, suggest a rotation-dependent transition in the magnetic properties of the atmosphere of 2MASS J22285440-1325178 the transition corresponds to approximately 10d, using previous observations of 2MASS J22285440-1325178. There is no correlation between the rotation period which is greater than 70 days, amplitude and flare rise time and equivalent duration. This show significant rotational period, modulation amplitude due to a star spot, as well as sharp flares are still witnessed throughout the observation.

Finally, the period of the star, flare amplitude and flare rise time and equivalent duration were found.

The most important and surprising conclusion deducible from this study of 2MASS J22285440-1325178 in the Kepler photometry is that the relative number of flare is probably much the same. The light curve shows significant flares which consistently spans the light curve for 70 days. 2MASS J22285440-1325178 is a variable star with frequent short and large flares throughout this observation period. Despite being observed at long cadence with approximately 30 minutes' exposure, 2MASS J22285440-1325178, sharp flares are still witnessed throughout the observation. Finally, the period of the star, flare amplitude and flare rise time and equivalent duration were found.

References

[1] Balona, L. A. (2015). Flare stars across the H–R diagram. *Monthly Notices of the Royal Astronomical Society*, 447 (3): 2714–2725.

[2] Dzombeta, K. and Percy, J. R. (2019). *Flare Stars: A Short Review*. Retrieved. 55 (2): 36-40.

[3] Hartman, J. D., Bakos, G, A., Noyes, R, W., Sipocz, B., Kovacs, G., Mazeh, T., … Pal, A. (2011). A Photometric Variability Survey of Field K and M Dwarf Stars with HATNet ´. *The Astronomical Journal*, 144 (166): 1–24.

[4] Alekseev, I. Y., Chalenko, V. E. and Shakhovsko, D. N. (2000). Rapid UBVRI Photometry of the Active Flare Stars EV Lac and AD Leo. *Astronomy Reports*, 44 (10): 777–783.

[5] Laher, R. R., Gorjian, V., Rebull, L. M., Masci, F. J., Fowler, J. W., Helou, G., … Law, N. M. (2012). Aperture Photometry Tool. *Publications of the Astronomical Society of the Pacific*, 124 (917): 737–763.

[6] Guarcello, M. G., Micela, G., Sciortino, S., López-Santiago, J., Argiroffi, C., Reale, F., … Stauffer, J. (2019). Simultaneous *Kepler* /K2 and *XMM-Newton* observations of superflares in the Pleiades. *Astronomy & Astrophysics*, 622 (23): *546-622*.

[7] Katsova, M. M. and Nizamov, B. A. (2018). Properties of Kepler Stars with the Most Powerful Flares. *Geomagnetism and Aeronomy*, 58 (7): 899–904.

[8] Roettenbacher, R. M. and Vida, K. (2018a). The Connection between Starspots and Flares on Main-sequence Kepler Stars. *The Astrophysical Journal*, 868 (1): 378-566.

[9] Roettenbacher, R. M. and Vida, K. (2018b). The Connection between Starspots and Flares on Main-sequence Kepler Stars. *The Astrophysical Journal*, 868 (1): 1–8.

[10] Haas, M. R., Batalha, N. M., Bryson, S. T., Caldwell, D. A., Dotson, J. L., Hall, J., … Van Clev, J. E. (2010). *Kepler Science Operations*. 234 (4): 88-89.

[11] Koch, D. G., Borucki, W. J., Basri, G., Batalha, N. M., Brown, T. M., Caldwell, D., … Wu, H. (2010). Kepler mission design, realized photometric performance, and early science. *Astrophysical Journal Letters*, 713 (5)*:* 456-501.

[12] Gershberg, R. E. and Knyazeva, S. (2005). Solar-Type Activity in Main-Sequence Stars. In G. Borner, Burkert, A, Burton, W B, Dopita, M A, Eckart, A, Encrenaz, T, … V. Trimble (Eds.), *Astronomy and Astrophysics Series* 87 (9): *876-879*.

[13] Güdel, M. and Nazé, Y. (2009). X-ray spectroscopy of stars. *Astronomy and Astrophysics Review*, 7 (2): 309–408.

[14] Tamazian, V. S. and Malkov, O. Y. (2014). Catalog of Binary UV Ceti Type Flare Stars. *ACTA ASTRONOMICA*, 64 (8): 359–369.

[15] Parimucha, Š., Dubovský, P., Vanko, M. and Cokino, M. (2016). Optical flare activity in the low-mass eclipsing binary GJ 3236. *Astrophys Space Sci*, 361 (302): 1–7.

[16] Bychkov, V. D., Bychkova, L. V., Madej, J. and Panferov, A. A. (2017). On global and local magnetic fields of flare stars with YZ CMi and OT Ser as examples. *Astrophysical Bulletin*, 8 (2): 178–183.

[17] Savanov, I. S. and Dmitrienko, E. S. (2018). Starspots and Activity of the Flare Star GJ 1243. *Astronomy Reports*, 62 (4): 273–280.

[18] Kowalski, A. F., Hawley, S. L., Holtzman, J. A., Wisniewski, J. P. and Hilton, E. J. (2010). A white light megaflare on the dM4.5e star YZ CMi. *Astrophysical Journal Letters*, 714 (1): 98-102.

[19] Melikian, N. D., Tamazian, V. S. and Samsonyan, A. L. (2011). Variation in the Flare Activity of the Star UV Ceti. *Astrofizika*, 54 (4): 469–475.

[20] Melikian, N. D. (2014). Spectra of Stellar Flares. Continuum Emission. *Astrofizika*, 57 (1): 77–89.

[21] Kozhevnikova, A. V, Kozhevnikov, V. P. and Alekseev, I. Y. (2018). Photospheric Spots and Flare on the active Dwarf Star FR Cnc. *Astrofizika*, 61 (1): 30–40.

[22] NASA, (2014). National Aeronautics and space Administration, 2 MASS (two-micron all sky survey) J18354A.

[23] Davenport, J. R. A., Hawley, S. L., Hebb, L., Wisniewski, J. P., Kowalski, A. F., Johnson, E. C., … Hilton, E. J. (2014a). kepler flares, the temporal morphology of white-light flares on gj 1243. *The Astrophysical Journal*, 797 (11): 122 - 30.

[24] Svanda and Karlick´y (2016). Different method to determine the power indices of the star. 605 (7): 76.

[25] Davenport, J. R. A. (2016). the kepler catalog of stellar flares. *The Astrophysical Journal*, 829 (1): 23 -25.

[26] Roettenbacher R. M and Vida K. (2018b). Finding flares in *Kepler* data using machine-learning tools. *Astronomy & Astrophysics*, 616-163.

[27] Gizis, J. E., Burgasser, A. J., Berger, E., Williams, P. K. G., Vrba, F. J., Cruz, K. L. and Metchev, S. (2013). Kepler monitoring of an L Dwarf I. the Photometric Period and White Light Flares. *Astrophysical Journal*, 779 2):172 -176.

[28] Makarov, Valeri V, Goldin, Alexey. (2017). Kepler Data on KIC 7341653: A Nearby M Dwarf with Montster Flares and a phase- coherent Variability.

[29] Giampapa, M. (1986). Stellar Analogs of Solar Activity: The Sun in A Stellar Context. In *The Sun, Solar Analogs and the Climate* (307–415).

[30] Davenport, J. R. A. (2018). *The shape of M dwarf flares in Kepler light curves*. (320): 128–133.

[31] Davenport, J. R. A., Hawley, S. L., Hebb, L., Wisniewski, J. P., Kowalski, A. F., Johnson, E. C., … Hilton, E. J. (2014b). *kepler* flares. ii. the temporal morphology of white-light flares on gj 1243. *The Astrophysical Journal*, 797 (2): 122.

[32] Han, X. L., Zhang, L., Pi, Q. and Wang, D. (2015). Lightcurve studies and magnetic activities of several eclipsing binaries. *Solar and Stellar Flares and Their Effects on Planets Proceedings IAU Symposium*, (320): 321–323.

[33] Barnes S. A., (2003). *Geomagnetism and Aeronomy* Astrophysical *Journal*, 80 (9): 333-350.

[34] Noyes R. W., Hartmann L. W., Baliunas S. L., Duncan D. K., Vaughan A. H., (1984). *Photometry and Flare Analysis Astrophysical Journal*, 45 (10): 279-763.